Biophysical Journal
Article

Biophysical Society

DPPC Bilayers in Solutions of High Sucrose Content

Mattia I. Morandi,[1] Mathieu Sommer,[1] Monika Kluzek,[1] Fabrice Thalmann,[1] André P. Schroder,[1] and Carlos M. Marques[1,*]
[1]Université de Strasbourg, CNRS, Institut Charles Sadron, UPR022, Strasbourg Cedex, France

ABSTRACT The properties of lipid bilayers in sucrose solutions have been intensely scrutinized over recent decades because of the importance of sugars in the field of biopreservation. However, a consensus has not yet been formed on the mechanisms of sugar-lipid interaction. Here, we present a study on the effect of sucrose on 1,2-dipalmitoyl-sn-glycero-3-phosphocholine bilayers that combines calorimetry, spectral fluorimetry, and optical microscopy. Intriguingly, our results show a significant decrease in the transition enthalpy but only a minor shift in the transition temperature. Our observations can be quantitatively accounted for by a thermodynamic model that assumes partial delayed melting induced by sucrose adsorption at the membrane interface.

INTRODUCTION

There is strong evidence that lipid membrane structures are well stabilized by small sugars (1,2). Disaccharides, and also other sugars, play a key role in preserving the structure and the functionality of biological membranes during periods of environmental stress (3). Besides their significant role in cellular regulation, carbohydrates also have a broad range of applications in biophysics and industrial research, particularly in the field of biopreservation and cryopreservation. Some sugars, such as sucrose and trehalose, are very efficient cryoprotectors (1,4,5). They have been shown to readily reduce the liquid-gel transition temperature T_m in highly dehydrated lipid bilayers and to increase the survivability of membranes undergoing freezing/thawing processes (6). Although this mechanism was initially associated with the ability of disaccharides to insert between adjacent lipid headgroups during dehydration and to hydrogen bond to them, an alternative model has been proposed that explains the observed effects in terms of sugar changes on the hydration repulsion (7).

Moreover, it has been proven that sugars play a role in the properties of hydrated bilayers. Döbereiner et al. (8) observed the strong influence of glucose on the spontaneous curvature of liposomes. Genova et al. (9) showed by fluctuation analysis that high concentrations of sucrose reduce the bending modulus k_b of stearoyl-oleoyl phosphatidylcholine giant vesicles by up to 25%, whereas Vitkova (10) found a 60% reduction using micropipette aspiration. Nagle (11) also showed by x-ray scattering that the bending rigidity of 1,2-dioleoyl-sn-glycero-3-phosphocholine bilayers is reduced, although it should be noted that recently the opposed effect has been reported (12).

Characteristic chain-melting temperatures T_m of phospholipid dispersions are known to increase as the activity of water decreases in the presence of increased solutes (13). Strauss et al. (13) found that the addition of more than 10% sucrose to hydrated multilamellar vesicles of 1,2-dipalmitoyl-sn-glycero-3-phosphocholine (DPPC) elevated the melting temperature by several degrees; they suggested a hydrogen-bonded sucrose network as the cause. Crowe and Crowe (14) found that several mono- and disaccharides raise T_m and broaden the main transition of large DPPC multilamellar vesicles (MLVs). However, the addition of sugars to unilamellar vesicles created multiple thermodynamic populations. High concentrations of trehalose, sucrose, and fructose created a low-temperature shoulder on the DPPC endotherm, indicating a second population with a lower T_m than that of pure hydrated DPPC.

Despite the observed influence of sugars on dry, semidry, and hydrated bilayers, relatively few studies have been conducted to understand the main effect of disaccharides on the lipid bilayer phase transition, and the mechanisms of interaction are yet to be understood. Although there is some agreement that high concentrations of sugar increase the transition temperature of the bilayer melting, the effect on the enthalpic contribution is quite discordant, reporting in certain cases no effect on the enthalpy of the transition and, in other studies, a significant decrease in energy. This

Submitted December 15, 2017, and accepted for publication April 2, 2018.
*Correspondence: marques@unistra.fr
Editor: Arne Gericke.
https://doi.org/10.1016/j.bpj.2018.04.003

discordance, likely due to differences in sample preparation methods, which lead to differing bilayer exposures to the sugars, calls for a more consistent approach.

In this work, we expose well-hydrated bilayers of DPPC to increasing concentrations of sucrose, up to 1.50 M. We probe the effect of sugar on the membrane phase behavior using a combination of differential scanning calorimetry (DSC) and Laurdan emission spectra to obtain structural and thermodynamical information. We also visualize changes in the phase behavior and kinetics of the transition by fluorescence microscopy of giant unilamellar vesicles (GUVs). Based on our experimental observations, we propose a thermodynamic model that quantitatively accounts for the effects of the interaction of sucrose with the lipid bilayer.

MATERIALS AND METHODS

Materials

Chloroform solutions of DPPC ($C_{40}H_{80}NO_8P$, $M_w = 734.039$, 10 mg/mL) and DMPC (1,2-dimyristoyl-sn-glycero-3-phosphocholine) ($M_w = 677.933$, 10 mg/mL) were purchased from Avanti Polar Lipid (Birmingham, AL). DiI stain (1,1′-dioctadecyl-3,3,3′,3′-tetramethylindocarbocyanine perchlorate, $C_{50}H_{97}ClN_2O_4$, $M_w = 933.8793$) was provided by Thermo Fisher Scientific (Waltham, MA) as a powder and dissolved in chloroform at 10 mg/mL final concentration. Sucrose ($C_{12}H_{22}O_{11}$ $M_w = 342.3$) and Laurdan (6-dodecanoyl-N,N-dimethyl-2-naphthylamine) were purchased from Sigma-Aldrich (Saint-Quentin, France). All chemicals had high purity and were used without further purification. The osmolarities of the sucrose solutions were measured with a cryoscopy osmometer Osmomat 030 (Gonotec, Berlin, Germany).

Liposomal preparation

2.5 mg of DPPC in chloroform was transferred to a glass vial, and organic solvent was evaporated using first an argon stream for 20 min, followed by 8 h of vacuum pumping. For fluorescence measurements, the lipids were stained with 1% mol Laurdan in chloroform before evaporation. The lipid film was then hydrated with aqueous solution (buffer or sucrose solution) at 70°C to reach the desired concentration and gently vortexed. The resulting MLV suspensions were sonicated for 15 min to disperse larger aggregates. Liposomal solutions remained stable over a period of days, as they were routinely checked with dynamic light scattering (Malvern Zetasizer Nano, Royston, United Kingdom).

Fluorimeter

3 mL of liposomal suspension stained with Laurdan of total concentration 3 mg/mL was placed in a quartz silica cuvette with a 1 mm path length. Acquisition of Laurdan emission spectra was performed with a Jobin Horiba FluoroMax equipped with a Peltier unit to control temperature. The excitation wavelength was set at 350 nm with a bandpass of 1 nm, and the emission was also recorded with slit of 1 nm. The solution was equilibrated at a given temperature for 10 min before each acquisition. For each sample, we performed two cycles of heating and cooling. Each spectrum acquisition was repeated three times on a new sample.

Generalized polarization (GP) was calculated using the standard expression provided by Parasassi (15):

$$GP = \frac{I_{440} - I_{490}}{I_{440} + I_{490}}, \quad (1)$$

where I_{440} and I_{490} are the values of the emitted intensity recorded at 440 and 490 nm, respectively.

DSC

The calorimetry measurements were performed using high sensitivity DSC (μDSC Setaram). The measurement cell was filled with the sonicated sample (MLVs at different concentrations of sucrose), whereas the reference cell was filled with the same sucrose solution. The heating rate was fixed at 0.5 K × min^{-1}, and the cooling rate was fixed at 0.3 K × min^{-1}. The system was equilibrated ~20 min before each heating or cooling ramp. The analysis of DSC data was performed using OriginPro 9.0 (OriginLab, Northampton, MA).

RESULTS AND DISCUSSION

Laurdan emission spectra

Fig. 1 illustrates the emission spectra of Laurdan for DPPC MLVs at different concentrations of sucrose at 20°C (Fig. 1 *A*) and 60°C (Fig. 1 *B*). Sucrose concentrations were chosen up to 1.5 M, thus covering well the relevant range for cryoprotection, i.e., 0.15–0.50 M (16,17). As shown also in Fig. S1, the spectra exhibit a continuous shift to longer wavelengths with increasing temperature while lipids undergo the gel-to-fluid transition. At 20°C, the maximal intensity is centered at 440 nm, corresponding to the signal associated with the gel phase (Fig. 1 *A*) (15). The figure further shows that the emission spectrum does not evolve with the sucrose concentration, remaining identical to that of DPPC in water, indicating that below T_m, the presence of sugar does not significantly modify the structure or order of the bilayer.

As temperature increases above the transition temperature T_m, we observe a decrease of total intensity together with a broadening of the emission spectrum, corresponding to an increasing red emission centered at 490 nm (Fig. 1 *B*). Such a decrease of intensity has been reported elsewhere (18). It is noteworthy that increasing concentrations of sucrose result in the persistence of a 440 nm shoulder in the emission spectra. This additional contribution is found to be dependent on the sucrose concentration and remains at any temperature above T_m. A Laurdan emission centered at 490 nm is attributed to a more relaxed Laurdan excited state, which would be favored by a more hydrated environment (19,20). Conversely, a contribution at 440 nm reflects a stiffer and/or less hydrated system surrounding the Laurdan naphthalene moiety. The evolution of GP with temperature and sucrose concentration appears to quantify the observed spectral changes, as shown in Fig. 2.

The values for DPPC in water are comparable to the values reported by Bagatolli et al. (21), as the GP decreases from 0.51 ± 0.02 for temperatures below T_m to −0.33 ± 0.01 for the fluid phase above T_m. The value for T_m extracted by interpolating the GP curves to determine the temperature at which GP = 0 is 41.5 ± 0.3°C, which is in good

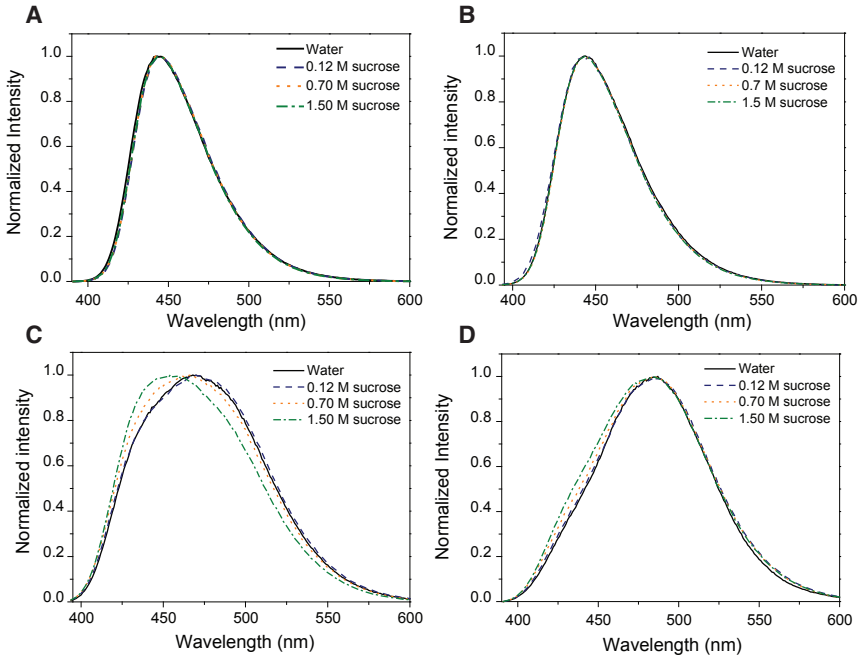

FIGURE 1 Comparison of emission curves of Laurdan for DPPC MLVs in pure water and 0.12, 0.70, and 1.50 M sucrose at (*A*) 20°C, (*B*) 30°C, (*C*) 42°C, and (*D*) 60°C. To see this figure in color, go online.

agreement with our DSC measurement of 41.3°C and with previously reported values (22). The GP transition from gel phase to liquid crystalline phase is sharp for any concentration of sucrose. A higher transition temperature is found by the same method for larger concentrations of sugar, as displayed in Table 1. The values of GP at temperatures below T_m are almost independent of sucrose content, although for temperatures near the transition (35 and 40°C), a slight increase of GP with an increasing amount of sugar can be observed; see the inset in Fig. 2.

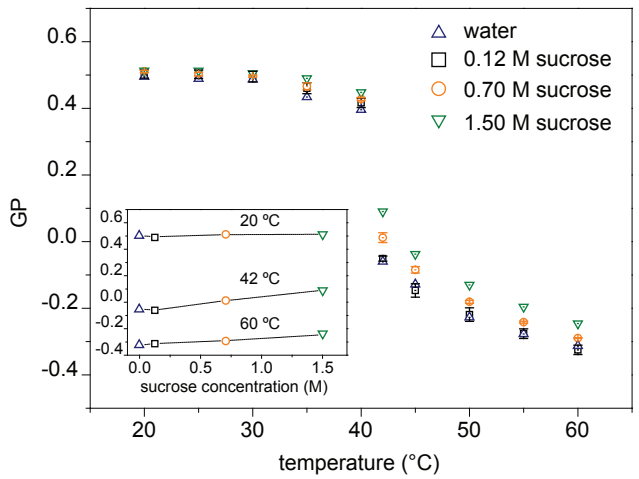

FIGURE 2 Variation of general polarization (GP) over temperature for multilamellar liposomes of DPPC formed in water and at different sucrose concentrations. A rise in GP values proportional to sucrose concentration is observed. Inset: the dependence of GP on sucrose concentration for 20°C, 42°C, and 60°C is shown. When not visible, error bars are smaller than symbol sizes. To see this figure in color, go online.

The inset also shows that above T_m in the fluid phase, GP values increase significantly with sucrose concentration, with GP increasing from −0.38 to −0.22 at 60°C for 1.50 M sucrose. Interestingly, the maximal variation of GP with sugar concentration can be observed at T_m, whereas for higher temperatures, the sensitivity of GP with respect to sugar content gradually decreases (Fig. 2, *inset*). The variation owed to the presence of sucrose appears to follow a linear dependence on sugar concentration in bulk for any analyzed temperature.

Laurdan is insoluble in water; therefore, any information from the emission spectra and GP arises entirely from the probe in the membrane. In lipid bilayers, the fluorescent moiety of Laurdan is located at the level of the glycerol backbone, and the emission shift upon change in temperature is due to a dipolar relaxation process (23). For MLVs formed in water, the red shift and decrease in GP generally associated with the phase transition are caused by a change in lipid packing, as the more disordered membrane allows for deeper penetration of the polar solvent molecules in the interfacial region.

TABLE 1 Summary of DSC Results for DPPC Liposomes in Sucrose Solution

Sucrose Concentration	T_m	$T_{1/2}$	ΔH	Laurdan T_m
[M]	[°C]	[°C]	[kJ/mol]	[°C]
0	41.8 ± 0.2	0.40 ± 0.01	38.5 ± 0.7	40.9 ± 0.6
0.39	41.9 ± 0.2	0.44 ± 0.01	33.6 ± 1.9	40.9 ± 0.4
0.7	42.1 ± 0.1	0.48 ± 0.01	27.9 ± 1.6	42.0 ± 0.5
1.5	42.7 ± 0.2	0.55 ± 0.02	23.9 ± 0.7	43.5 ± 0.4

Variations of emission spectra and GP, such as those shown in this study, have been reported before in cases of high ionic strength or in the presence of cations in the buffer for dimyristoylphosphatidylglycerol liposomes (24,25). In these studies, the effect was due to changes in lipid packing upon electrostatic attraction caused by ionic charges. Despite sucrose being highly polar, our results show that when it is present in high concentration, the Laurdan emission spectra display a small decrease in the polarity of the solvent surrounding the probe naphtalene moiety (18). Conversely, increased GP values in the presence of sugar are linked to a lower mobility for water or a smaller number of water molecules around the Laurdan naphthalene moiety.

Two possible mechanisms can be invoked to explain such an effect: 1) tighter lipid packing of the membrane, as observed for example in liquid-ordered (L_o) phases in the presence of cholesterol, and 2) depletion of water molecules at the lipid headgroup region, which reduces the emission shift of Laurdan.

Simulations and previous experimental studies showed that the adsorption of sugar to the membrane leads to a smaller number of molecules around the lipid headgroup (5,26–28). These results are consistent with our GP data, which show a progressive reduction of water molecules surrounding the Laurdan naphthalene moiety, resulting in higher GP values.

DSC

Fig. 3 reports DSC results on DPPC MLVs hydrated with water, and 0.39, 0.70, and 1.50 M sucrose. Fig. 3 *A* shows the raw data; integration of the area under the peak around T_m gives the energy associated with the transition from the gel to liquid crystalline phases, which is related to the local packing of the membrane upon melting (29).

The intensity of the peak decreases with increasing amounts of sugar, and the center of the peak shifts to slightly higher temperatures with the sucrose concentration. However, the curves remain sharp, indicating that the transition is still highly cooperative. Broadening of the peaks is usually associated with disruption of lipid packing and cooperativity (30), as reported by Mannock et al. (31) for cholesterol. Here, such large broadening is not present, suggesting no significant disruption of the number of lipids participating in the transition cooperatively.

The enthalpy (ΔH), transition temperature (T_m), and mid-height width ($T_{1/2}$) of the peaks are summarized in Table 1. For DPPC membranes formed in pure water, the enthalpy of the transition is 38.5 kJ/mol with temperature T_m at 41.8°C, which is in good agreement with previously reported values (32,33). A significant drop in enthalpy in the presence of sucrose is observed, with a final value of 23.9 kJ/mol at 1.50 M sucrose. A drop in sucrose concentration of DPPC enthalpy of transition has been observed previously by Chowdhry and Chen (32,33). Our values are in good agreement with the variation of 10.9 kJ/mol for 1 M sucrose measured by Chowdhry. Chen, however, reported a drop of 11.6 kJ/mol earlier at 0.2 M sucrose, which we did not observe.

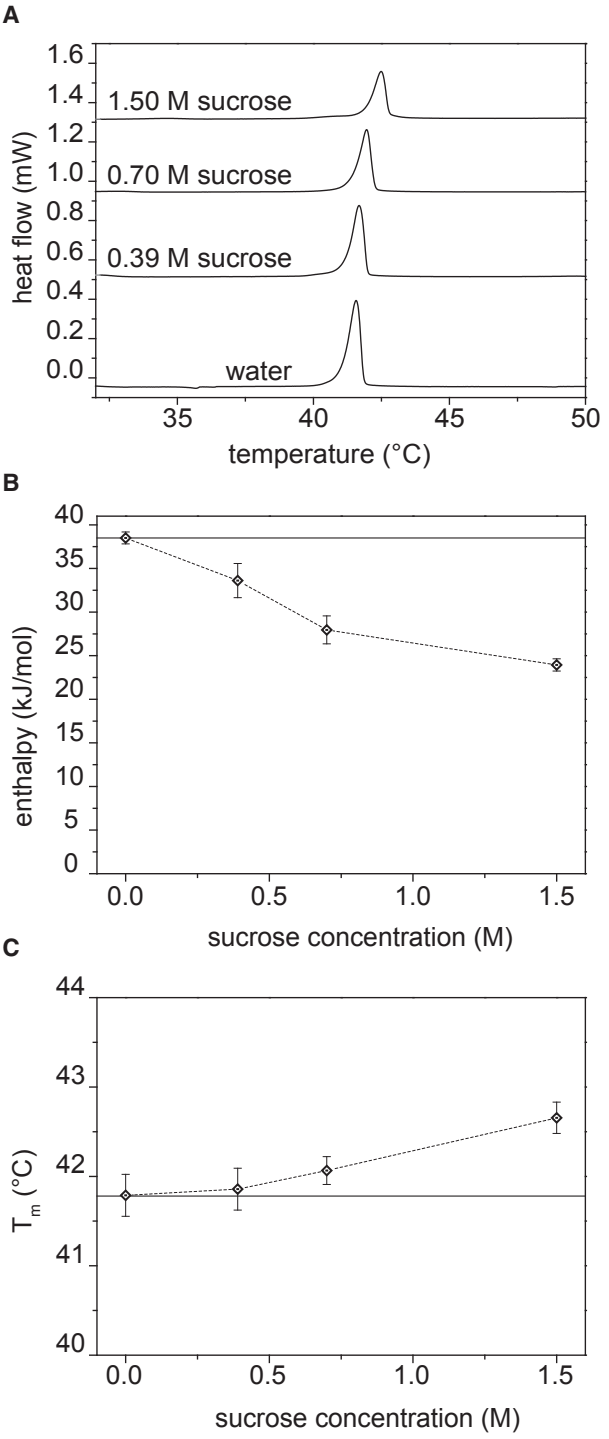

FIGURE 3 Summary of DSC results for DPPC MLVs at different concentrations of sucrose. (*A*) A DSC calorimetric signal is shown. (*B*) Decreases in enthalpy at different sucrose concentrations are shown. (*C*) Variation of T_m with sucrose concentration is shown. In both (*B*) and (*C*), the full straight line represents the initial value in pure water, and the dashed lines connect the experimental points.

Surprisingly, our results show a nonlinear trend for the enthalpy change with sucrose concentration (Fig. 3 *B*). The enthalpy dropping rate slows down at 1.50 M, suggesting a saturation of the sucrose effect on the membrane transition. This saturation could be linked to a maximal adsorption of sucrose at the surface, as it was measured with electron spin echo envelope modulation by Konov et al. (34), who reported Langmuir adsorption isotherms of sucrose on DPPC bilayers.

The transition temperature for DPPC increases only slightly with sucrose concentration, with a final value of 42.7°C for 1.50 M of sucrose. These changes in T_m, albeit small, are in good agreement with the increase of 0.6°C at 1 M reported by Chowdhry, measured via calorimetry (32). Stümpel et al. (35) also observed a shift of ~1°C in the T_m of DMPC MLVs in the presence of 1.17 M sucrose. Similar effects have been reported on DMPC vesicles (36). Other studies instead reported little or no changes in T_m, contrary to our results (33). As a matter of fact, many studies report variations in the T_m of lipid bilayers upon interaction with macromolecules located either at the surface or in the hydrophobic region of the membrane (37,38). An increase in the transition temperature is generally linked to a tighter packing of the lipids, with different possible causes. In this study, we argue that the observed shift of T_m to higher temperatures is due to a dehydration of the lipid bilayer. Indeed, sugar molecules, by accumulating on the membrane surface, substitute water molecules from the first hydration layer, increasing the transition temperature. This is in agreement with our observation of the Laurdan emission spectra, which indicate a decrease in the number of water molecules at the water-membrane interface.

In poorly hydrated (20% water content) DPPC vesicles, Gabrielle-Delmont (39) reported an enthalpy drop and a small T_m shift comparable to our observations. Such low hydration conditions, however, lead to a high temperature peak in the DSC curves, which is a contribution we do not see for our experimental conditions in which minimal water content is ~60% (or 1.50 M) sucrose. The effect of substitution of water molecules by sucrose cannot therefore be reduced to simple bilayer dehydration. Finally, we observe a slight increase of $T_{1/2}$, which is consistent with the values reported by Chen (33).

Thermodynamic model

We now attempt to rationalize our experimental observations on the interaction of sucrose with a DPPC bilayer by means of a thermodynamic model.

In discussing the interaction between dry bilayers and sugars, a frequent model is the water replacement hypothesis, which postulates direct hydrogen bonding between sugars and phospholipids (1). By creating H bonds with lipid headgroups, sugars keep lipids separated in the liquid phase upon dehydration. In some cases, the hypothesis considers the sugars to be able to penetrate the interfacial region of the membrane and therefore keep the lipids apart. Although our data do support the removal of water molecules from the membrane, the water replacement hypothesis cannot explain both the increase in T_m and the decrease of enthalpy.

Another proposed model is the hydration forces explanation (40,41), which assumes no direct interaction between sugars and lipids. Sugars and nonspecific volumetric and osmotic effects are the causes of change in the bilayer phase transition. This model has been able to quantitively predict changes in the transition temperature (7,42); however, the variations of enthalpy reported here and in previous studies have not been explained.

A thermodynamic model that would fully explain the observed phenomena should include the following: 1) a mild increase in the transition temperature, 2) a significant drop in enthalpy, and 3) a decrease in the cooperativity of the transition. As we will see below, the last point is required to reconcile the apparent contraction of the first two without invoking some unknown reason for an almost perfect balance of the enthalpic and entropic variations.

We propose a model in which the adsorption of sucrose at the membrane surface locally dehydrates the lipid bilayer, resulting in the formation of clusters with intrinsically different transition temperatures; see Fig. 4. As change of state occurs, only a fraction of the lipids participate, resulting in a lower enthalpic contribution and a higher effective melting temperature, coupled with a broader peak.

To interpret our data, we use a formalism previously introduced to reproduce the calorimetry of pure and binary lipid systems (43–45). This description is akin to an Ising spin model, where the spin represents the internal state (phase) of the lipid. Based on (44), the configurational energy difference of the reference gel state for a pure lipid bilayer is given by:

$$\Delta\mathcal{H} = N_l(\Delta h - T\Delta s) + JN_{gl}, \tag{2}$$

where N_l is the number of lipids in the liquid phase, Δh is the enthalpy of melting per molecule at the transition, Δs is the corresponding entropy contribution, J is the cooperativity parameter, and N_{gl} is the number of gel-liquid lipid pairs in contact. A penalty J is counted every time a nearest-neighbor pair of lipids is found with different internal states, i.e., a mismatched pair.

We assume that sucrose molecules in contact with lipid molecules slightly modify the enthalpy and entropy of melting while decreasing the cooperativity parameter (the mismatch energy). A full derivation of our model can be found in the Supporting Materials and Methods. Following this approach, the configurational energy difference is defined as follows:

$$\begin{aligned}\Delta\mathcal{H} = {} & N_l(\Delta h - T\Delta s) + N_l'(\Delta h' - T\Delta s') \\ & + J'N_{gl}' + JN_{gl} + J''N_{gl}''\end{aligned}, \tag{3}$$

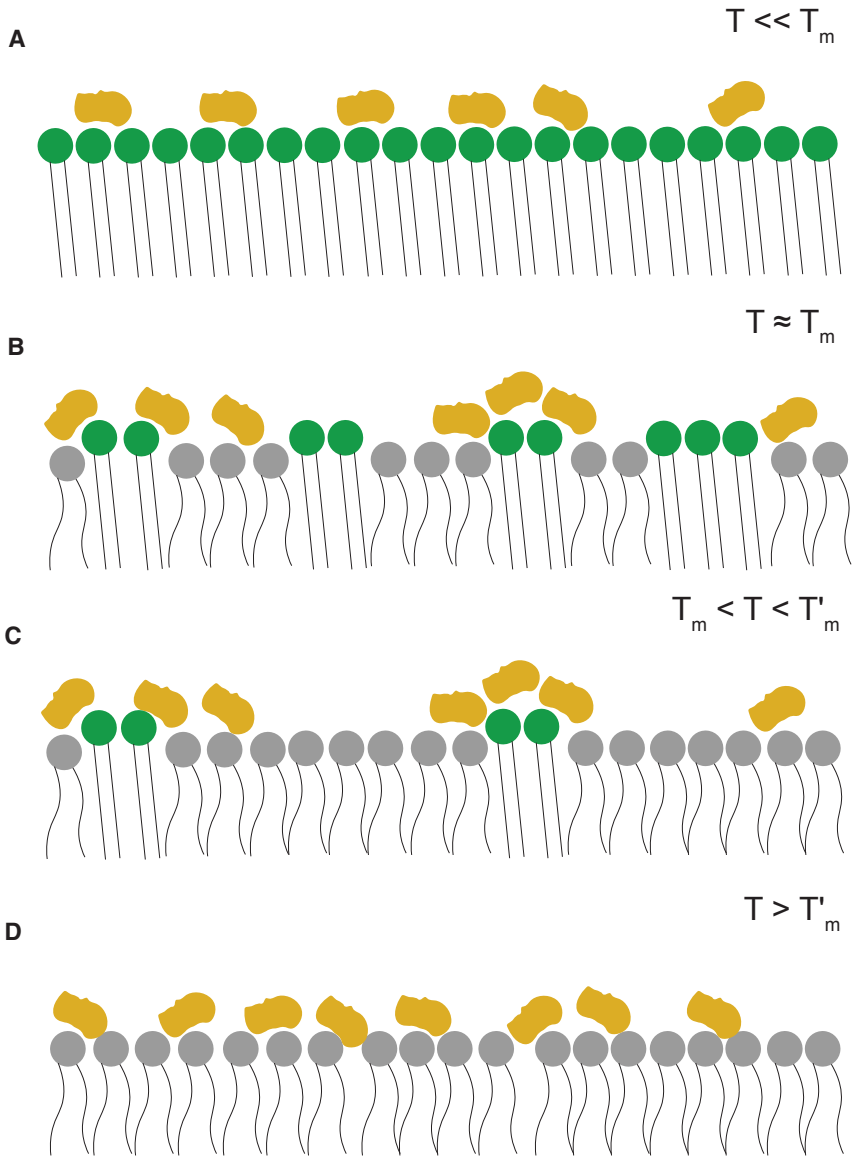

FIGURE 4 Schematic representation of the interaction of sucrose with the lipid bilayer at different temperatures. (*A*) Below T_m, the lipid bilayer is in the S_o phase, with sucrose molecules excluded from the interfacial region of the lipid headgroup. (*B*) At temperatures near T_m, the membrane undergoes a gel-to-fluid transition in which clusters of lipid melt into the fluid phase. The lipids that interact less with sucrose melt at T_m, whereas lipids dehydrated by interaction with saccharides will have higher effective transition temperatures T'_m. (*C*) In the intermediate region between T_m and T'_m, the lipids interacting with sucrose are still in the gel phase. (*D*) Above T'_m, the membrane is completely in the fluid phase, with sucrose molecules adsorbed on the membrane and penetrating the interfacial region. To see this figure in color, go online.

where JN_{gl} represents, as in Eq. 2, the internal mismatch energy between neighboring lipids in different states. For the case without sucrose, $J'N'_{gl}$ is the mismatch energy when neighboring lipids in different states are both in contact with sucrose, and $J''N''_{gl}$ is the mismatch energy when only one lipid is in contact with sucrose. $N_{gl}+N'_{gl}+N''_{gl}$ is the total number of gel-fluid lipid pairs.

We now introduce the probability σ for a lipid to be in contact with a sucrose molecule, assuming that σ is constant and controlled by the concentration of sucrose in solution. The number of lipids in the gel and liquid states thus depends on the site coverage σ and the probabilities $p, p\prime$ for a lipid to be in a specific state. The number of lipids is determined by

$$\begin{aligned} N_l &= N(1-\sigma) \times p \\ N_g &= N(1-\sigma)(1-p) \end{aligned} \tag{4}$$

for free lipids and

$$\begin{aligned} N'_l &= N \times \sigma \times p' \\ N'_g &= N \times \sigma(1-p') \end{aligned} \tag{5}$$

for sucrose-bound lipids. To estimate the interaction terms, we use a mean-field approximation involving the probabilities $p, p\prime, \sigma$ and the average coordination number z of lipid molecules in each plane leaflet:

$$\begin{aligned} N_{gl} &= (1-\sigma)^2 \times \frac{zN}{2} \times 2p(1-p) \\ N''_{gl} &= 2\sigma(1-\sigma)\frac{zN}{2}[p(1-p')+p'(1-p)] \\ N'_{gl} &= \sigma^2 \times \frac{zN}{2} \times 2p'(1-p'). \end{aligned} \tag{6}$$

The average enthalpy difference can be expressed using the above mean-field approximation as follows:

$$\langle \Delta H \rangle(T) = N[p(1-\sigma)\Delta h + p'\sigma\Delta h'] + J_{\text{tot}}, \quad (7)$$

where J_{tot} is the sum of all the cooperativity terms listed in Eq. 3. As pointed out in (44), the respective enthalpy and entropy contributions to J_{tot} are arbitrary. We assume here that J_{tot} is purely of enthalpic origin. Fortunately, it turns out that $\langle \Delta H \rangle$ depends only marginally on this assumption.

Adding to the configurational energy (3) the mean-field configurational entropy given by

$$\begin{aligned} -\mathcal{S}/k_B = N[&\sigma\ln(\sigma) + (1-\sigma)\ln(1-\sigma) + \sigma[p'\ln(p') \\ &+(1-p')\ln(1-p')] \\ &+(1-\sigma)[p\ln(p) + (1-p)\ln(1-p)]] \end{aligned} \quad (8)$$

and minimizing $\langle \Delta\mathcal{H} \rangle - T\mathcal{S}$ with respect to p and $p\prime$ leads to the following set of self-consistent equations:

$$\begin{aligned} &\ln\left(\frac{p}{1-p}\right) - \frac{\mathcal{N}_A \Delta h}{RT_m^2}(T - T_m) + \tilde{J}(1-\sigma)(1-2p) \\ &\qquad +\tilde{J}''\sigma(1-2p') = 0; \\ &\ln\left(\frac{p'}{1-p'}\right) - \frac{\mathcal{N}_A \Delta h}{RT_m^2}(T - T'_m) + \tilde{J}'\sigma(1-2p') \\ &\qquad +\tilde{J}''(1-\sigma)(1-2p) = 0. \end{aligned} \quad (9)$$

As explained in Supporting Materials and Methods, we performed a numerical calculation using our model for a coordination number $z = 6$ with the following parameter values: $T_m \simeq 315$ K, $T'_m \simeq 320$ K, with J corresponding to 200 cal/mol, J', J'' corresponding to 100 cal/mol, and $\mathcal{N}_A \Delta h = \mathcal{N}_A \Delta h' = 56$ kJ•mol^{-1}. As a result, the enthalpy (7) increases sharply around the nominal melting transition temperature. We retain the change in enthalpy across a ± 5 K temperature interval centered around 315 K as representative of the experimental heat adsorbed at the transition. The inflection point of $\Delta H_{\text{tot}}(T)$ with respect to temperature gives us the apparent melting temperature. No attempt was made to reproduce the shape of the measured excess-specific heat curve, given the mean-field character of our treatment.

Our coverage parameter σ was adjusted to the experimental conditions by comparing the theoretical value of σ required to obtain the enthalpy reduction measured for given mass concentrations of sucrose, as shown in Fig. S2, with an approximately linear variation being found between σ and the sucrose concentration. The experimental changes in enthalpy (Fig. 5 *A*) and the shift in transition temperatures (Fig. 5 *B*) are found to be well described by this theoretical model, thus supporting its main assumptions.

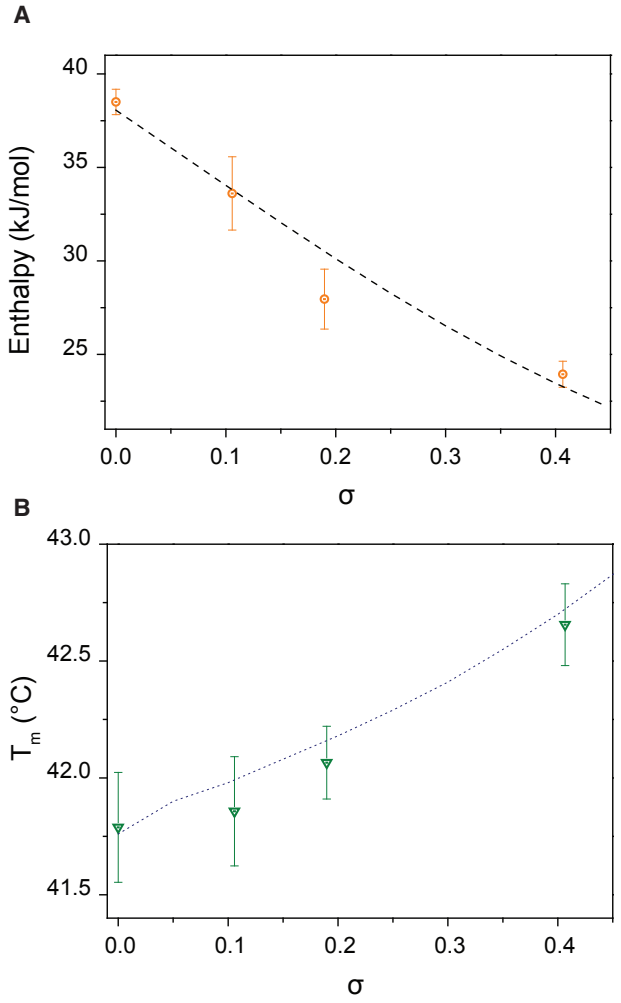

FIGURE 5 (*A*) Experimental values of ΔH for the DPPC gel-to-liquid transition at different concentrations of sucrose (*circles*), and theoretical predictions from the thermodynamics model (*dotted line*). (*B*) Experimental values of T_m for the DPPC gel-to-liquid transition are shown at different concentration of sucrose (*triangles*), and theoretical predictions from the thermodynamics model are also shown (*dotted line*). To see this figure in color, go online.

CONCLUSIONS

In this study, we have shown that sucrose can alter the gel-liquid phase transition of DPPC lipid bilayers, slightly increasing T_m while lowering the enthalpy of the transition by a significant amount. Our experimental results bring together complementary techniques to probe a consistent set of samples, thus reducing the previous dispersion of conclusions likely because of the different degrees of exposure of the bilayers to the sugars as a consequence of different preparation methods. We not only clarify previous observations concerning the effects of sugars in well-hydrated lipid bilayers of DPPC but also raise puzzling questions about the mechanisms of sugar-bilayer interactions. Our spectrometric results based on GP measurements of Laurdan do point to a dehydration of the membrane interfacial region.

However, if the main action of the sugar was to dehydrate the bilayers, then a much larger shift of T_m to larger values would be expected. We propose here an explanation for this conundrum by a mechanism of partially delayed transition. More specifically, we assume that lipids in contact with sugars have their transition shifted to higher temperatures, whereas the others behave in an unperturbed manner. As our model quantitatively predicts based on these assumptions, this suppresses the measurable heat release around the calorimetric maximum, shifting the value of the maximum by a few degrees.

The excellent agreement between our model and the thermodynamic and spectrometric data reported in this article suggests that further investigations of the bilayer properties must be conducted. In particular, it would be important to inspect bilayer behavior at the optical length scales with lipid platforms such as GUVs. Although for technical reasons we were not able to perform such experiments for DPPC GUVs, we did perform preliminary experiments for DMPC GUVs in solutions with different sucrose concentrations; see Supporting Materials and Methods. As our results with DMPC show, the sugar reduces the width of the metastable region above T_m, where out-of-equilibrium domains are observed. Such reduction is compatible with a sugar-induced decrease of the mismatch energy between lipids in the gel and liquid states, which is a key ingredient of our model. Also, the interaction between the sugars and the lipids might induce different kinetics for sugar-free and sugar-bound lipids that could be probed not only by a systematic study of the influence of the cooling and heating rates on the transition but also by changing the nature of the sugars.

SUPPORTING MATERIAL

Supporting Materials and Methods and six figures are available at http://www.biophysj.org/biophysj/supplemental/S0006-3495(18)30440-5.

AUTHOR CONTRIBUTIONS

M.I.M., M.S., and M.K. performed the experiments. F.T. developed the theoretical model. F.T., A.P.S., and C.M.M. designed and managed the project. M.I.M., F.T., A.P.S., and C.M.M. contributed to the writing of the article.

ACKNOWLEDGMENTS

The ISO9001 Characterization Platform of Institut Charles Sadron is gratefully acknowledged for access to μDSC.

M.I.M., M.K., F.T., A.P.S., and C.M.M. acknowledge funding from the European FP7-MSCA International Training Network SNAL 608184 (Smart Nano-Objects for Alteration of Lipid Bilayers) for support for this work.

SUPPORTING CITATIONS

References (46–59) appear in the Supporting Material.

REFERENCES

1. Crowe, L. M., D. S. Reid, and J. H. Crowe. 1996. Is trehalose special for preserving dry biomaterials? *Biophys. J.* 71:2087–2093.
2. Crowe, J. H., L. M. Crowe, …, F. Tablin. 2001. The trehalose myth revisited: introduction to a symposium on stabilization of cells in the dry state. *Cryobiology.* 43:89–105.
3. Yancey, P. H., M. E. Clark, …, G. N. Somero. 1982. Living with water stress: evolution of osmolyte systems. *Science.* 217:1214–1222.
4. Crowe, J. H., L. M. Crowe, …, C. Aurell Wistrom. 1987. Stabilization of dry phospholipid bilayers and proteins by sugars. *Biochem. J.* 242:1–10.
5. Luzardo, M. C., F. Amalfa, …, E. A. Disalvo. 2000. Effect of trehalose and sucrose on the hydration and dipole potential of lipid bilayers. *Biophys. J.* 78:2452–2458.
6. Harrigan, P. R., T. D. Madden, and P. R. Cullis. 1990. Protection of liposomes during dehydration or freezing. *Chem. Phys. Lipids.* 52:139–149.
7. Lenné, T., C. J. Garvey, …, G. Bryant. 2009. Effects of sugars on lipid bilayers during dehydration–SAXS/WAXS measurements and quantitative model. *J. Phys. Chem. B.* 113:2486–2491.
8. Döbereiner, H. G., O. Selchow, and R. Lipowsky. 1999. Spontaneous curvature of fluid vesicles induced by trans-bilayer sugar asymmetry. *Eur. Biophys. J.* 28:174–178.
9. Genova, J., A. Zheliaskova, and M. D. Mitov. 2006. The influence of sucrose on the elasticity of SOPC lipid membrane studied by the analysis of thermally induced shape fluctuations. *Colloids Surf. A Physicochem. Eng. Asp.* 282–283:420–422.
10. Vitkova, V., J. Genova, …, I. Bivas. 2006. Sugars in the aqueous phase change the mechanical properties of lipid mono- and bilayers. *Mol. Cryst. Liq. Cryst. (Phila. Pa.).* 449:95–106.
11. Nagle, J. F., M. S. Jablin, …, K. Akabori. 2015. What are the true values of the bending modulus of simple lipid bilayers? *Chem. Phys. Lipids.* 185:3–10.
12. Nagle, J. F., M. S. Jablin, and S. Tristram-Nagle. 2016. Sugar does not affect the bending and tilt moduli of simple lipid bilayers. *Chem. Phys. Lipids.* 196:76–80.
13. Strauss, G., P. Schurtenberger, and H. Hauser. 1986. The interaction of saccharides with lipid bilayer vesicles: stabilization during freeze-thawing and freeze-drying. *Biochim. Biophys. Acta.* 858:169–180.
14. Crowe, L. M., and J. H. Crowe. 1991. Solution effects on the thermotropic phase transition of unilamellar liposomes. *Biochim. Biophys. Acta.* 1064:267–274.
15. Parasassi, T., E. K. Krasnowska, …, E. Gratton. 1998. Laurdan and Prodan as polarity-sensitive fluorescent membrane probes. *J. Fluoresc.* 8:365–373.
16. Rodrigues, J. P., F. H. Paraguassú-Braga, …, L. C. Porto. 2008. Evaluation of trehalose and sucrose as cryoprotectants for hematopoietic stem cells of umbilical cord blood. *Cryobiology.* 56:144–151.
17. Anchordoguy, T. J., A. S. Rudolph, …, J. H. Crowe. 1987. Modes of interaction of cryoprotectants with membrane phospholipids during freezing. *Cryobiology.* 24:324–331.
18. Parasassi, T., M. Di Stefano, …, E. Gratton. 1994. Influence of cholesterol on phospholipid bilayers phase domains as detected by Laurdan fluorescence. *Biophys. J.* 66:120–132.
19. De Vequi-Suplicy, C. C., C. R. Benatti, and M. T. Lamy. 2006. Laurdan in fluid bilayers: position and structural sensitivity. *J. Fluoresc.* 16:431–439.
20. Bagatolli, L. A., E. Gratton, and G. D. Fidelio. 1998. Water dynamics in glycosphingolipid aggregates studied by Laurdan fluorescence. *Biophys. J.* 75:331–341.
21. Bagatolli, L. A., B. Maggio, …, G. D. Fidelio. 1997. Laurdan properties in glycosphingolipid-phospholipid mixtures: a comparative fluorescence and calorimetric study. *Biochim. Biophys. Acta.* 1325:80–90.
22. Jacobson, K., and D. Papahadjopoulos. 1975. Phase transitions and phase separations in phospholipid membranes induced by changes in

temperature, pH, and concentration of bivalent cations. *Biochemistry.* 14:152–161.

23. Vequi-Suplicy, C. C., K. Coutinho, and M. T. Lamy. 2015. New insights on the fluorescent emission spectra of Prodan and Laurdan. *J. Fluoresc.* 25:621–629.
24. Lúcio, A. D., C. C. Vequi-Suplicy, …, M. T. Lamy. 2010. Laurdan spectrum decomposition as a tool for the analysis of surface bilayer structure and polarity: a study with DMPG, peptides and cholesterol. *J. Fluoresc.* 20:473–482.
25. Riske, K. A., R. P. Barroso, …, M. T. Lamy. 2009. Lipid bilayer pretransition as the beginning of the melting process. *Biochim. Biophys. Acta.* 1788:954–963.
26. Sum, A. K., R. Faller, and J. J. de Pablo. 2003. Molecular simulation study of phospholipid bilayers and insights of the interactions with disaccharides. *Biophys. J.* 85:2830–2844.
27. Roy, A., R. Dutta, …, N. Sarkar. 2016. A comparative study of the influence of sugars sucrose, trehalose, and maltose on the hydration and diffusion of DMPC lipid bilayer at complete hydration: investigation of structural and spectroscopic aspect of lipid-sugar interaction. *Langmuir.* 32:5124–5134.
28. Pereira, C. S., R. D. Lins, …, P. H. Hünenberger. 2004. Interaction of the disaccharide trehalose with a phospholipid bilayer: a molecular dynamics study. *Biophys. J.* 86:2273–2285.
29. Demetzos, C. 2008. Differential scanning calorimetry (DSC): a tool to study the thermal behavior of lipid bilayers and liposomal stability. *J. Liposome Res.* 18:159–173.
30. Marsh, D., A. Watts, and P. F. Knowles. 1977. Cooperativity of the phase transition in single- and multibilayer lipid vesicles. *Biochim. Biophys. Acta.* 465:500–514.
31. Mannock, D. A., R. N. Lewis, and R. N. McElhaney. 2006. Comparative calorimetric and spectroscopic studies of the effects of lanosterol and cholesterol on the thermotropic phase behavior and organization of dipalmitoylphosphatidylcholine bilayer membranes. *Biophys. J.* 91:3327–3340.
32. Chowdhry, B. Z., G. Lipka, and J. M. Sturtevant. 1984. Thermodynamics of phospholipid-sucrose interactions. *Biophys. J.* 46:419–422.
33. Chen, C. H., D. S. Berns, and A. S. Berns. 1981. Thermodynamics of carbohydrate-lipid interactions. *Biophys. J.* 36:359–367.
34. Konov, K. B., D. V. Leonov, …, S. A. Dzuba. 2015. Membrane-sugar interactions probed by pulsed electron paramagnetic resonance of spin labels. *J. Phys. Chem. B.* 119:10261–10266.
35. Stümpel, J., W. L. Vaz, and D. Hallmann. 1985. An X-ray diffraction and differential scanning calorimetric study on the effect of sucrose on the properties of phosphatidylcholine bilayers. *Biochim. Biophys. Acta.* 821:165–168.
36. Fabrie, C. H., B. de Kruijff, and J. de Gier. 1990. Protection by sugars against phase transition-induced leak in hydrated dimyristoylphosphatidylcholine liposomes. *Biochim Biophys Acta.* 1024:380–384.
37. Ali, S., S. Minchey, …, E. Mayhew. 2000. A differential scanning calorimetry study of phosphocholines mixed with paclitaxel and its bromoacylated taxanes. *Biophys. J.* 78:246–256.
38. Bothun, G. D. 2008. Hydrophobic silver nanoparticles trapped in lipid bilayers: size distribution, bilayer phase behavior, and optical properties. *J. Nanobiotechnology.* 6:13.
39. Grabielle-Madelmont, C., and R. Perron. 1983. Calorimetric studies on phospholipidwater systems. *J. Colloid Interface Sci.* 95:471–482.
40. Koster, K. L., Y. P. Lei, …, G. Bryant. 2000. Effects of vitrified and nonvitrified sugars on phosphatidylcholine fluid-to-gel phase transitions. *Biophys. J.* 78:1932–1946.
41. Wolfe, J., and G. Bryant. 1999. Freezing, drying, and/or vitrification of membrane- solute-water systems. *Cryobiology.* 39:103–129.
42. Lenné, T., C. J. Garvey, …, G. Bryant. 2010. Kinetics of the lamellar gel-fluid transition in phosphatidylcholine membranes in the presence of sugars. *Chem. Phys. Lipids.* 163:236–242.
43. Doniach, S. 1978. Thermodynamic fluctuations in phospholipid bilayers. *J. Chem. Phys.* 68:4912–4916.
44. Heimburg, T., and R. L. Biltonen. 1996. A Monte Carlo simulation study of protein-induced heat capacity changes and lipid-induced protein clustering. *Biophys. J.* 70:84–96.
45. Heimburg, T. 2007. Thermal Biophysics of Membranes. Wiley-VCH, Weinheim, Germany.
46. Bagatolli, L. A., and E. Gratton. 1999. Two-photon fluorescence microscopy observation of shape changes at the phase transition in phospholipid giant unilamellar vesicles. *Biophys. J.* 77:2090–2101.
47. Hirst, L. S., A. Ossowski, …, R. L. Selinger. 2013. Morphology transition in lipid vesicles due to in-plane order and topological defects. *Proc. Natl. Acad. Sci. USA.* 110:3242–3247.
48. Klymchenko, A. S., and R. Kreder. 2014. Fluorescent probes for lipid rafts: from model membranes to living cells. *Chem. Biol.* 21:97–113.
49. Baumgart, T., G. Hunt, …, G. W. Feigenson. 2007. Fluorescence probe partitioning between Lo/Ld phases in lipid membranes. *Biochim. Biophys. Acta.* 1768:2182–2194.
50. Chen, D., and M. M. Santore. 2014. Large effect of membrane tension on the fluid-solid phase transitions of two-component phosphatidylcholine vesicles. *Proc. Natl. Acad. Sci. USA.* 111:179–184.
51. Metso, A. J., H. Zhao, …, P. K. Kinnunen. 2005. Observation of the main phase transition of dinervonoylphosphocholine giant liposomes by fluorescence microscopy. *Biochim. Biophys. Acta.* 1713:83–91.
52. Jørgensen, K., and O. G. Mouritsen. 1995. Phase separation dynamics and lateral organization of two-component lipid membranes. *Biophys. J.* 69:942–954.
53. Crowe, J. H., L. M. Crowe, and D. Chapman. 1984. Preservation of membranes in anhydrobiotic organisms: the role of trehalose. *Science.* 223:701–703.
54. Angelova, M. I., and D. S. Dimitrov. 1986. Liposome electroformation. *Faraday Discuss. Chem. Soc.* 81:303–311.
55. Moiset, G., C. A. López, …, S. J. Marrink. 2014. Disaccharides impact the lateral organization of lipid membranes. *J. Am. Chem. Soc.* 136:16167–16175.
56. Goldstein, R. E., and S. Leibler. 1989. Structural phase transitions of interacting membranes. *Phys. Rev. A Gen. Phys.* 40:1025–1035.
57. Jerala, R., P. F. Almeida, and R. L. Biltonen. 1996. Simulation of the gel-fluid transition in a membrane composed of lipids with two connected acyl chains: application of a dimer-move step. *Biophys. J.* 71:609–615.
58. Ivanova, V. P., and T. Heimburg. 2001. Histogram method to obtain heat capacities in lipid monolayers, curved bilayers, and membranes containing peptides. *Phys. Rev. E Stat. Nonlin. Soft Matter Phys.* 63:041914.
59. Fisher, M. E. 1967. The theory of equilibrium critical phenomena. *Rep. Prog. Phys.* 30:615.

Biophysical Journal, Volume *114*

Supplemental Information

DPPC Bilayers in Solutions of High Sucrose Content

Mattia I. Morandi, Mathieu Sommer, Monika Kluzek, Fabrice Thalmann, André P. Schroder, and Carlos M. Marques

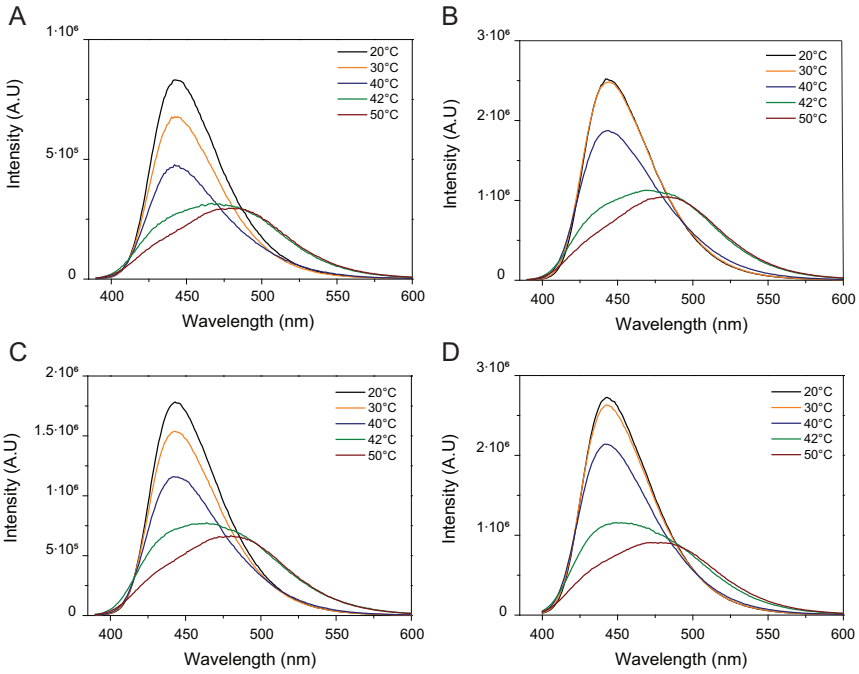

Figure S1: Comparison of emission curves of Laurdan for DPPC MLVs formed in (A) water, (B) 0.12 M sucrose, (C) 0.70 M sucrose and (D) 1.50 M sucrose at 20°C (black line), 35°C (orange line), 42°C(blue line), 50°C(green line) and 60°C (red line).

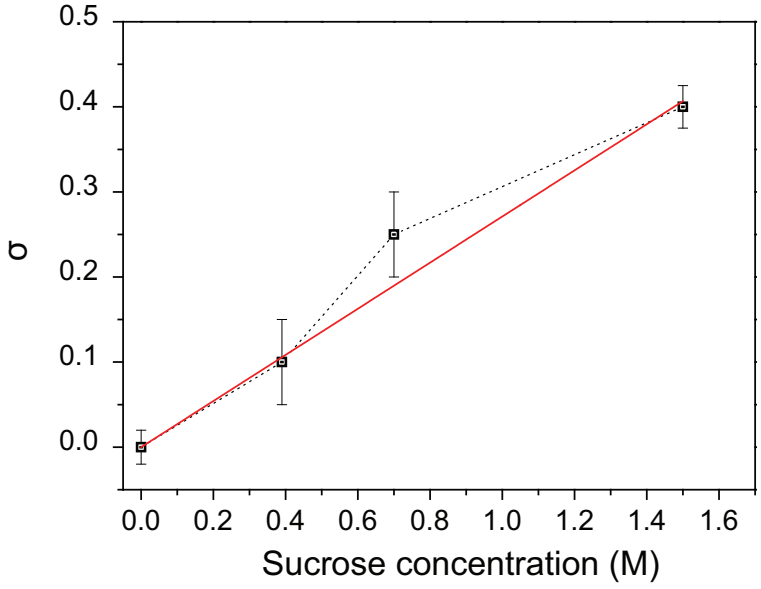

Figure S2: Dependence of sucrose coverage σ on the sucrose concentration (black squares connected by dashed lines) and linear fitting (red line). Each value of σ, which is a parameter of our model, was found by fitting the model to the experimentally obtained values of transition enthalpy.

Preparation of giant unilamellar vesicles

GUVs were prepared by electroformation following the protocol introduced by Angelova (54). Briefly, 5 μL of 2 mg/mL solution of DMPC stained with 1% mol of diI in chloroform were spread on each cathode of a custom made electroformation stage. The stage was kept under vacuum for at least one hour to ensure complete evaporation of solvent and the lipid film was subsequently hydrated using the necessary solution (water or sucrose at different concentrations) at 55 °C.

A sinusoidal electric field (1 V peak-peak, 10 Hz) was applied for one hour while keeping the sample heated above the transition temperature. The resulting GUV suspension was kept at 20 °C (water bath) during two hours prior to use to ensure complete stabilization of the sample. Vesicles were used on the same day of preparation.

Optical Microscopy

Imaging of GUVs labelled with DiI was performed using an epifluorescence microscope Nikon Eclipse TE2000-E equipped with a x60, water immersion, NA 1.2, Nikon objective, and a Diagnostic Instrument, NI-1800, black and white camera. Prior to any observation, GUVs were submitted to an osmotic shock: the sample was diluted with $\sim$5% volume of pure water. As a consequence, GUVs underwent swelling, resulting in the removal of potential membrane tubes connected to the membrane. The samples were kept at 5 °C for at least two hours after preparation to ensure complete transition to gel (also called S_o) phase. Prior to experimental observation, GUVs were let to stabilize at 20 °C for at least one hour. 100 mL of a GUV dispersion were placed in a custom-made heating stage through which we could control the temperature of the sample with a precision of $\pm$1 °C. Sample was stabilized for at least one hour for each temperature, before acquiring images.

Giant unilamellar vesicles

Giant unilamellar vesicles of DMPC were observed in epifluorescence to probe the membrane phase behavior at the micrometric scale, at temperatures below and above T_m, known to be 25°C . Typical vesicle morphologies for each sucrose concentration at different temperatures are summarized in Fig. S3, together with statistics of phase separation.

At 20°C, DMPC vesicles appear homogenous, whatever the sucrose content. The corrugations of the membrane and steep angle defects have been previously reported for DMPC vesicles and are characteristic of a S_o gel phase (40, 41). Increasing the temperature to 25°C results in phase separation displayed by fluorescent probe partitioning. DiI has been shown to readily partition into the fluid phase (42,43), therefore the black domains observed in the micrographs are gel-phase domains in a liquid phase. In pure water, domains are still observed for both 30°C and 35°C, however they gradually decrease in size with increasing temperature. The partitioning of DiI also decreases as the contrast between domains becomes less sharp. At 40°C the membrane is in a liquid phase and displays homogenous fluorescence.

Vesicles formed in 0.20 M sucrose display a similar behavior to GUVs formed in water, however gel domains readily disappear at a lower temperature. Moreover the partitioning of DiI gradually diminishes already at 30°C, and at 35°C contrast between domains and fluid phase is very low.

For 0.39 M sucrose we observe narrower window of coexistence, since domains are only visible at 25°C, whereas at 30°C or higher a single homogeneous fluid phase is present.

It appears that for any given sucrose concentration and temperature, GUVs exhibit a similar fraction of S_o domains. This is summarized in Fig. S3B, where the temperature window of phase coexistence for

each concentration of sucrose is clearly vizualized. Though different domain typologies were observed in the GUVs, namely stripes, hexagonal and irregular, they all can be attributed to different states of tension of the individual vesicle, and be systematically associated with S_o domains (46).

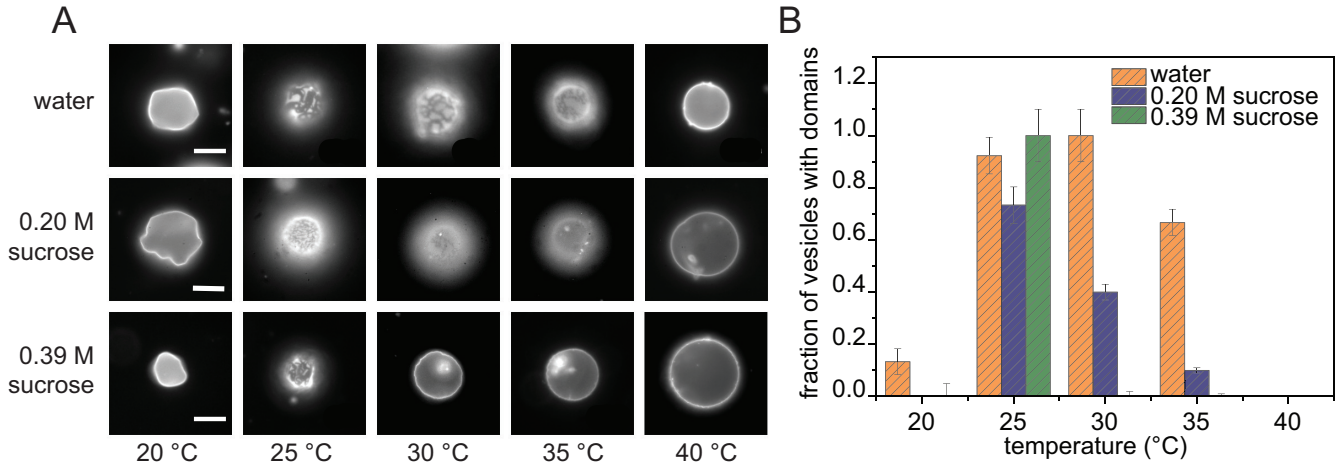

Figure S3: Summary of sucrose effects on GUVs formed with DMPC. A) Typical GUV phase behavior for DMPC in water, 0.20 M and 0.39 M sucrose in the temperature interval [20°C - 40°C]. Scale bar is 10 μm. B) Fraction of DMPC GUVs with domains for each system at the different temperatures displayed in A).

These measurements reveal that, for pure DMPC GUVs, a large temperature interval of phase coexistence exists, which has not been reported before in giant vesicles experiments. Although phase coexistence is expected to appear around T_m (45), the persistence of gel domains at higher temperatures may indicate that metastability is produced (46), possible because of the low rate of heating employed in the experimental setup.

The suppression by sucrose of phase coexistence for temperatures above T_m can be interpreted as a lowering of the energy involved with gel-liquid contact. The size of gel domains in liquid phase is mainly driven by the minimization of the energy involved with hydrophobic mismatch (such as a S_o/L_d coexistence) (46). Several studies have proposed that sucrose can alter the head-head distance in lipid bilayers under low hydration conditions (1, 47). Sucrose is likely to act as a reliever of hydrophobic mismatch allowing for smaller domains existence, by protecting the portion of chains exposed by the mismatch (55). It is thus possible that the presence of sugar enhances the dissolution of domains or reduces the lifetime of metastable states.

Derivation of a thermodynamic model for sucrose-lipid interaction

Cooperativity in the lipid main transition

It is assumed that the gel and fluid phases exchange their stability at a coexistence temperature T_m by means of a first order transition mechanism. Let us introduce the number of lipids N, the total Gibbs free-energies G_l, G_g, the enthalpies H_l, H_g and entropies S_l, S_g in the fluid and gel phases.

Molecular quantities are defined as $g_l = G_l/N$, $g_g = G_g/N$, $h_l = H_l/N$, $h_g = H_g/N$, $s_l = S_l/N$, $s_g = S_g/N$. Finally, we introduce the differences $\Delta g = g_l - g_g$, $\Delta h = h_l - h_g$, $\Delta s = s_l - s_g$

between the high (fluid) and low (gel) temperature phases. We denote by T the absolute temperature, and $\beta = 1/(k_B T)$ the inverse temperature factor. The probability of occurrence of a phase is proportional to $\exp(-\beta G)$. As the Gibbs free-energy scales with the number of lipids, phases cannot coexist except but in a narrow temperature interval centered around T_m.

A standard thermodynamic relation states that

$$\frac{\mathrm{d}(\beta G)}{\mathrm{d}\beta} = G + \beta \frac{\mathrm{d}}{\mathrm{d}\beta} G = G - T \frac{\mathrm{d}}{\mathrm{d}T} G = G + TS = H. \tag{S1}$$

On the other hand, at the coexistence temperature $\Delta G(T_m) = 0$. One can expand to first order in $T - T_m$ the difference in Gibbs free-energy

$$\beta \Delta G \simeq (\beta - \beta_m) \Delta H_m \simeq -\frac{T - T_m}{k_B T_m^2} \Delta H_m. \tag{S2}$$

The probability of occurrence of the gel and liquid phases reads

$$\begin{aligned} p_l(N, \beta) &= \frac{e^{-\beta G_l}}{e^{-\beta G_l} + e^{-\beta G_g}} = \frac{1}{1 + e^{\beta N \Delta g}}; \\ p_g(N, \beta) &= \frac{e^{-\beta G_g}}{e^{-\beta G_l} + e^{-\beta G_g}} = \frac{1}{1 + e^{-\beta N \Delta g}}. \end{aligned} \tag{S3}$$

The transition takes place on a temperature interval ΔT given by $\beta N \Delta g = N \Delta T \Delta h_m / k_B T_m^2 \sim 1$. It is inversely proportional to N. To provide a phenomenological description of the melting transition, one introduces a cooperativity number N_c as the effective number of lipids that share the same internal state. The system is then treated as an assembly of N/N_c "bundles" changing state independently, with $N/N_c \gg 1$. The equilibrium enthalpy at temperature T is given by:

$$H(T) = N(p_l(N_c, T) h_l + p_g(N_c, T) h_g) = N(p_l(N_c, T) \Delta h + h_g). \tag{S4}$$

where liquid-gel mismatch energy contributions are neglected and h_l and h_g are taken independent of temperature at the vicinity of the transition. Then

$$\begin{aligned} \frac{\mathrm{d}H}{\mathrm{d}T} &= N \Delta h \frac{\mathrm{d}p_l}{\mathrm{d}T}, \\ &= N \Delta h \frac{-e^{\beta N_c \Delta g}}{(1 + e^{\beta N_c \Delta g})^2} \frac{\mathrm{d}\beta N_c \Delta g}{\mathrm{d}T}, \\ &= N N_c \frac{(\Delta h)^2}{k_B T^2} \frac{e^{\beta N_c \Delta g}}{(1 + e^{\beta N_c \Delta g})^2}, \\ &= n N_c \frac{(\mathcal{N}_A \Delta h)^2}{4RT^2} \frac{1}{\cosh(\beta N_c \Delta g / 2)^2}, \end{aligned} \tag{S5}$$

with $\mathcal{N}_A$ the Avogadro number, $\mathcal{N}_A \Delta h$ the molar enthalpy change at the transition, n the number of moles of lipids.

The peak maximum is at $\Delta g = 0$, $C_{p,max} = \mathrm{d}H/\mathrm{d}T|_{T=T_m} = nRN_c(\mathcal{N}_A \Delta h)^2/(4R^2T^2)$, from which N_c can be expressed in terms of molar quantities

$$N_c = \frac{C_{p,\max}}{n} \frac{4RT_m^2}{(\mathcal{N}_A \Delta h)^2} = 4 \left(\frac{C_{p,max}}{nR} \right) \left(\frac{RT_m}{\mathcal{N}_A \Delta h} \right)^2. \tag{S6}$$

Phenomenology of the lipid main transition

A simple insightful treatment of the lipid main transition was introduced by Doniach, and improved by several authors (51, 52, 55, 57, 58). It is based on a scalar order parameter showing two preferred values, one corresponding to the gel state, and the other to the fluid state. This statistical model can be implemented in practice by assigning binary variables (Ising spins) to the fixed vertices of a two dimensional lattice. Reference (52) presents in detail the historical development of the model.

In this approach, lipid molecules spontaneously adopt either a gel or a fluid conformation, depending on external thermodynamic conditions (temperature, but also isotropic pressure and membrane tension). In the Ising language, this is achieved by applying a uniform temperature (pressure, tension) dependent magnetic field that vanishes precisely at the coexistence temperature T_m, where fluid and gel are observed with equal probability. Additional nearest neighbor couplings (J parameters) are introduced to enforce cooperativity. Above a critical J_c value, the system shows phase coexistence and metastability, with thermal hysteresis upon heating and cooling cycles. Below the critical value, the system state evolves smoothly and reversibly with temperature. The latter case is therefore suitable to describe most experimental situations corresponding to a regular and reversible thermal capacity curve with a finite width, determined *e.g.* in differential scanning calorimetry (DSC) experiments.

There is some freedom left in deciding whether the binary state is assigned to a whole lipid or just a lipid chain, or which lattice is most representative (the hexagonal lattice seeming the most appropriate), with all models in the end able to describe the observed behavior (57). Several Monte-Carlo studies were shown to successfully account for various situations of interest (56).

To explain the main features of sucrose induced changes in the DPPC melting transition, we implement one such model and solve it by means of a mean-field approximation. Each binary state takes a value 0 (gel) or 1 (fluid) and describes a single lipid molecule internal state. The average internal value is therefore a real number p comprised between 0 and 1, which is readily interpreted as the probability to find a lipid molecule in the fluid conformation. For a given microscopic configuration, one introduces a configurational energy

$$\Delta\mathcal{H} = N_l(\Delta h - T\Delta s) + JN_{gl}, \tag{S7}$$

as the difference between the actual system state, and a reference state where all lipids would be in the gel state. N_l and N_{gl} are respectively the number of lipids in fluid state, and the number of lattice bonds linking lipids in a different state (state mismatch). J is the mismatch gel-fluid state penalty parameter. The quantity $\Delta\mathcal{H}$ determines the probability of the microscopic state, proportional to $\exp(-\beta\Delta\mathcal{H})$. Note that it is unusual to deal with temperature dependent "Hamiltonians" in statistical physics. The approach used here means that a coarse-graining step is performed by averaging over the inner conformations of each lipid molecule, while partitioning them into two broad classes (gel and fluid state). Eq. (S7) is something of an intermediate quantity between the true (molecular) microscopic energy and the macroscopic Gibbs free-energy.

$\beta\Delta\mathcal{H}$ can be expanded around the coexistence temperature:

$$\beta\Delta\mathcal{H} = -\frac{\mathcal{N}_A\Delta h}{RT_m^2}(T - T_m)N_l + \frac{\mathcal{N}_A J}{RT_m}N_{gl}. \tag{S8}$$

The Gibbs free-energy associated to the configurational energy above reads in the large N limit:

$$\beta\Delta G = \beta\langle\Delta\mathcal{H}\rangle - \mathcal{S}/k_B, \tag{S9}$$

where appears the entropy $\mathcal{S}$ associated to the many internal gel-fluid microscopic configurations of the system. The above expression can be expressed at mean-field level by introducing the probability p of

finding each lipid in the fluid state, and the average coordination z of a site in the lattice (average number of neighboring lipid molecules, 6 for an hexagonal lattice). It reads

$$\beta\Delta G = -\frac{\mathcal{N}_A\Delta h}{RT_m^2}(T-T_m)Np + \frac{\mathcal{N}_A J}{RT_m}zNp(1-p) + N[p\ln(p)+(1-p)\ln(1-p)]. \tag{S10}$$

The $\mathcal{S}/k_B = -N[p\ln(p)+(1-p)\ln(1-p)]$ expression is characteristic of the statistical entropy of N independent binary variables. The mean-field self-consistent equations result from minimizing $\beta\Delta G$ with respect to p, in order to find the best compromise between the number of configurations $\exp(\mathcal{S}/k_B)$ and the energy penalty $\langle\Delta\mathcal{H}\rangle$. One obtains

$$\ln(p) - \ln(1-p) + \frac{\mathcal{N}_A J}{RT_m}z(1-2p) - \frac{\mathcal{N}_A\Delta h}{RT_m^2}(T-T_m) = 0, \tag{S11}$$

or equivalently

$$\frac{p}{1-p} = \exp\left(\frac{\mathcal{N}_A\Delta h}{RT_m^2}(T-T_m) + \frac{\mathcal{N}_A J}{RT_m}z(2p-1)\right). \tag{S12}$$

Self-consistent equations are trivially satisfied by

$$p(T) = \frac{\exp\left(\frac{\mathcal{N}_A\Delta h}{RT_m^2}(T-T_m)\right)}{1+\exp\left(\frac{\mathcal{N}_A\Delta h}{RT_m^2}(T-T_m)\right)} \tag{S13}$$

at vanishing coupling $J=0$, and must be numerically solved in the general case.

There is freedom in deciding if the interaction term $-Jzp(1-p)$ is of enthalpic or entropic origin. Assuming that J is enthalpic and does not depend on temperature T, one derives the mean-field enthalpy difference

$$\Delta H(T) = Np(T)\Delta h + JzNp(T)(1-p(T)) \tag{S14}$$

that can be compared with the experimental DSC thermograms once the solution of eq. (S12) is obtained. Moreover, one observes that, irrespective of the choice done regarding the interaction term, the difference $\Delta H(p=1) - \Delta H(p=0)$ reaches the expected limit value $N\Delta h$, corresponding to the total latent heat upon melting completely the system from the gel to the fluid state.

Introducing the dimensionless coupling $\tilde{J} = \frac{\mathcal{N}_A J}{RT_m}z$, one finds that the critical value separating reversible and temperature hysteresis is $\tilde{J}_c = 2$ in the mean-field approximation. A quite sharp specific heat peak can therefore be obtained with $\tilde{J}_c \simeq 1.94$.

In the practical situation of a DPPC bilayer, when assigning binary variables to lipid molecules (not chains), treating lipids as basic degrees of freedom coupled with $\tilde{J}_c = 1.94$, and taking $\mathcal{N}_A\Delta h$ equal to the experimental value $38\ \mathrm{kJ\cdot mol^{-1}}$ (9.1 kcal $\cdot\mathrm{mol}^{-1}$) leads to a non negligible amount of the minor component into the major component around the location of the phase transition. This means that the area under the peaked curve $\mathrm{d}\Delta H/\mathrm{d}T$ on a 10°C temperature interval centered around $T_m = 273.15 + 41.8 = 314.95$K gives a value 28 kJ·mol^{-1}, smaller than the experimental one. This is inherent to the "Ising" like treatment of the internal degrees of freedom, and is also true for Monte-Carlo "exact" sampling of the configurations. To get around this shortcoming, one can decide on a phenomenological ground to assign a larger value to the constant $\mathcal{N}_A\Delta h$. We found that at mean field level, with $\tilde{J}_c = 1.94$, the correct $\Delta H(T_m+5) - \Delta H(T_m-5) = 38\ \mathrm{kJ\cdot mol^{-1}}$ value is recovered for $\mathcal{N}_A\Delta h = 56\ \mathrm{kJ\cdot mol^{-1}}$ (13.4 kcal·mol^{-1}). There is then 16% of fluid lipid at $T_m - 5 = 36.8$°C and 84% at $T_m + 5 = 46.8$°C.

Influence of the sucrose on the gel transition

Increasing concentrations of sucrose in solution lead to a noticeable drop in latent heat (area under the specific heat curve) with only a tiny increase in the appearent melting temperature (of the order of 1 K).

In first order phase transitions, the coexistence temperature T_m coincides with the ratio $\Delta h/\Delta s$. If the sucrose was only acting on changing the enthalpy jump $\Delta h'$, then keeping the melting temperature constant by 1 part in 300 would require a quasi-perfect matching of the entropy variation $\Delta s'$, with $T_m = \Delta h/\Delta s \simeq \Delta h'/\Delta s'$. On the other hand, it is well known that lipid melting temperature is extremely sensitive to molecular details. Perdeuteration of the DPPC alkyl chains, for instance, lowers the transition temperature by 4°C. Shifting one C16 fatty acid chain link with glycerol from *sn*-2 to *sn*-3 position has the same consequence. Going from *cis* to *trans* double bond insaturations raise the melting transition of DOPC by 60 K.

If one thinks of the action of sucrose as simply dehydrating the lipid headgroups, then a strong elevation of the melting transition temperature would be expected. Yet, the observed change goes in this direction, but in much weaker proportions. In addition, hydrophilic sucrose molecules are not really expected to interact with the bulk of hydrophobic alkyl chains region, which is where the largest part of the contribution to the enthalpy change Δh is expected to arise from.

Drops in latent heat at the transition can be alternatively explained by the presence of domains. If one assumes that in the presence of sucrose, lipids get separated into sucrose-depleted and sucrose enriched domains, and that only sucrose depleted domains melt as usual, with other domains remaining in the gel phase, then the result would also be a neat decrease in experimental latent heat. However, here is no clear reason for such domains to form, and this mechanism lacks experimental support.

We propose here an alternative mechanism where sucrose adsorbs indistinctly in the gel and fluid phases. Lipids that are in close contact with sucrose molecules are assumed to melt at a slightly higher temperature T'_m, and more importantly, to behave in a less cooperative way than in pure lipid water solutions. This could be justified for instance by saying that gel-fluid mismatch configurations are eased by surrounding sucrose molecules.

Adapting the previous model, the configurational energy becomes

$$\Delta\mathcal{H} = (\Delta h - T\Delta s)N_l + (\Delta h' - T\Delta s')N'_l + JN_{gl} + J'N'_{gl} + J''N''_{gl}, \tag{S15}$$

with N_l the number of free lipids in fluid state, N'_l the number of lipid in fluid state in contact with sucrose, N_{gl} the number of unlike gel-fluid free lipid pairs, N'_{gl} the number of unlike gel-fluid lipid pairs, both in contact with sucrose and N''_{gl} the number of unlike gel-fluid pairs with one lipid free and one lipid in contact with sucrose, J, J', J'' being the corresponding mismatch penalties.

We assume now that the probability for a lipid to be in contact with sucrose is σ, that p is the average probability of finding free lipids in fluid state, and p' the average probability of finding lipids in contact with sucrose in fluid state. The average configurational energy can be expressed in the mean-field limit.

$$\begin{aligned}\langle\beta\Delta\mathcal{H}\rangle &= -\frac{\mathcal{N}_A\Delta h}{RT_m^2}(T - T_m)(1-\sigma)Np - \frac{\mathcal{N}_A\Delta h}{RT_m^2}(T - T'_m)\sigma Np' \\ &\quad + N\tilde{J}(1-\sigma)^2p(1-p) + N\tilde{J}'\sigma^2p'(1-p') \\ &\quad + N\tilde{J}''\sigma(1-\sigma)[p(1-p') + p'(1-p)]\end{aligned} \tag{S16}$$

where for simplicity we assume $\Delta h \simeq \Delta h'$, $T_m \simeq T'_m$ at the first order of the temperature expansion. The mean field configurational entropy then becomes:

$$\begin{aligned} -\mathcal{S}/k_B &= N\Big[\sigma p' \ln(\sigma p') + \sigma(1-p')\ln[\sigma(1-p')] \\ &\quad +(1-\sigma)p\ln[(1-\sigma)p] + (1-\sigma)(1-p)\ln[(1-\sigma)(1-p)]\Big], \\ &= N\Big[\sigma\ln(\sigma) + (1-\sigma)\ln(1-\sigma) + \sigma[p'\ln(p') + (1-p')\ln(1-p')] \\ &\quad +(1-\sigma)[p\ln(p) + (1-p)\ln(1-p)]\Big]. \end{aligned} \tag{S17}$$

The Gibbs free-energy $\beta\Delta G(p,p',\sigma,T) = \langle\beta\Delta\mathcal{H}\rangle - \mathcal{S}/k_B$ must now be minimized with respect to p and p'. We do not perform a minimization over σ because we assume σ imposed by the sucrose molarity ([Sucrose]) of the hydrating solution.

The self-consistent equations become

$$\begin{aligned} \ln\left(\frac{p}{1-p}\right) - \frac{\mathcal{N}_A\Delta h}{RT_m^2}(T-T_m) + \tilde{J}(1-\sigma)(1-2p) + \tilde{J}''\sigma(1-2p') &= 0; \\ \ln\left(\frac{p'}{1-p'}\right) - \frac{\mathcal{N}_A\Delta h}{RT_m^2}(T-T'_m) + \tilde{J}'\sigma(1-2p') + \tilde{J}''(1-\sigma)(1-2p) &= 0. \end{aligned} \tag{S18}$$

With the numerical solution for $p(T), p'(T)$ determined, the temperature dependent enthalpy is readily obtained from eq. (S16).

In practice, equations (S18) are solved for each temperature T using the Newton-Raphson iteration scheme, starting initially from the exact solution at $\tilde{J} = \tilde{J}' = \tilde{J}'' = 0$, and iteratively converged for increasing values of the coupling constant. Below critical coupling $\tilde{J}_c = 2$, the method is fast and accurate.

An interesting behavior is obtained for the following choice of parameters:

- $T_m = 273.15 + 41.8$ K, $T'_m = 273.15 + 41.8 + 5.0$ K,
- $\tilde{J} = 1.94$; $\tilde{J}' = \tilde{J}'' = 0.97$,
- $\mathcal{N}_A\Delta h = \mathcal{N}_A\Delta h' = 56$ kJ $\cdot$ mol^{-1}.

The three graphs below explains how the decreased cooperativity mechanism works:

0.1 Connection with previous work and correspondence with the usual Ising model

Ising variables are usually binary variables s taking the values ± 1. The order parameter $m = \langle s\rangle$ is a real number comprised between -1 and 1. The correspondence between p and m is

$$m = 2p - 1 \Leftrightarrow p = (1+m)/2. \tag{S19}$$

At T_m, eq. (S12) can be rewritten

$$\frac{1+m}{1-m} = \exp(\tilde{J}m), \tag{S20}$$

which can be inverted as

$$m = \frac{e^{\tilde{J}m} - 1}{e^{\tilde{J}m} + 1} = \tanh(\tilde{J}m/2). \tag{S21}$$

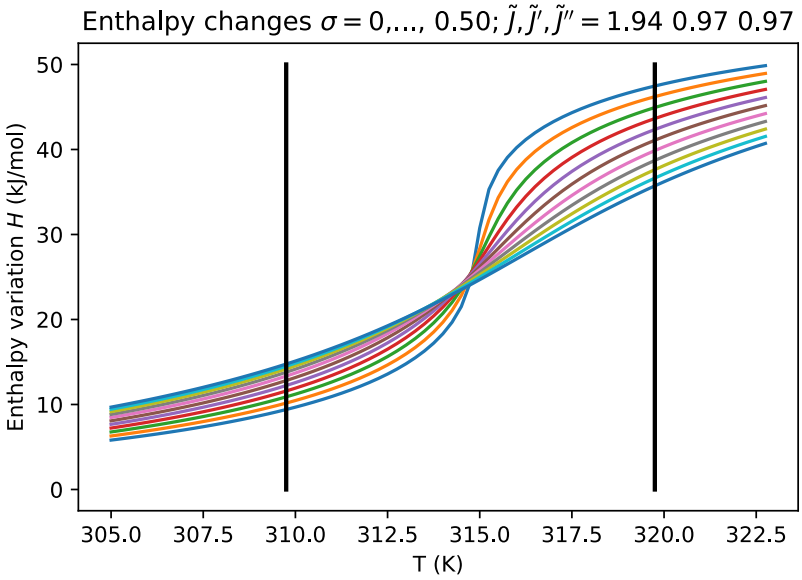

Figure S4: Enthalpy variation with temperature as σ increases from 0 to 0.5. We integrate the area under the specific heat curve from $T_m - 5$ K to $T_m + 5$ K.

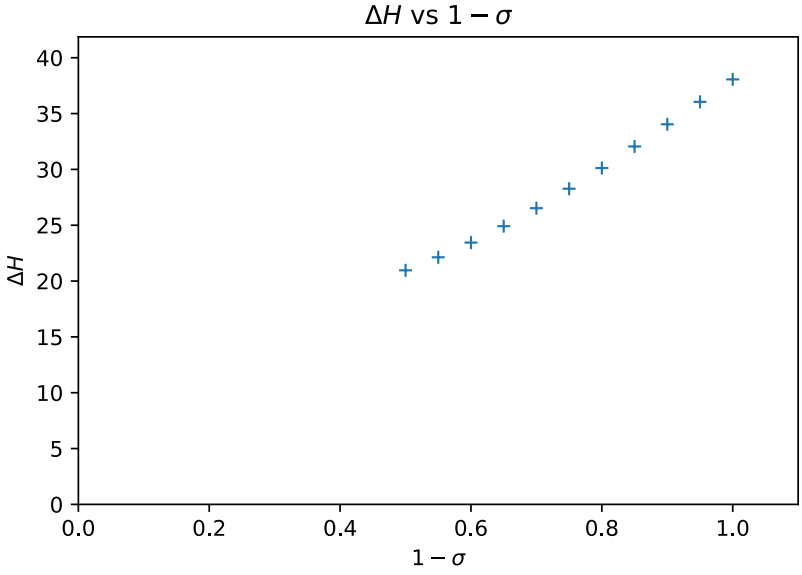

Figure S5: Resulting enthalpy change vs $1 - \sigma$ (pure water at the right of the graph). We note that for the selected values, the ΔH curves seem initially to decrease linearly with $1 - \sigma$.

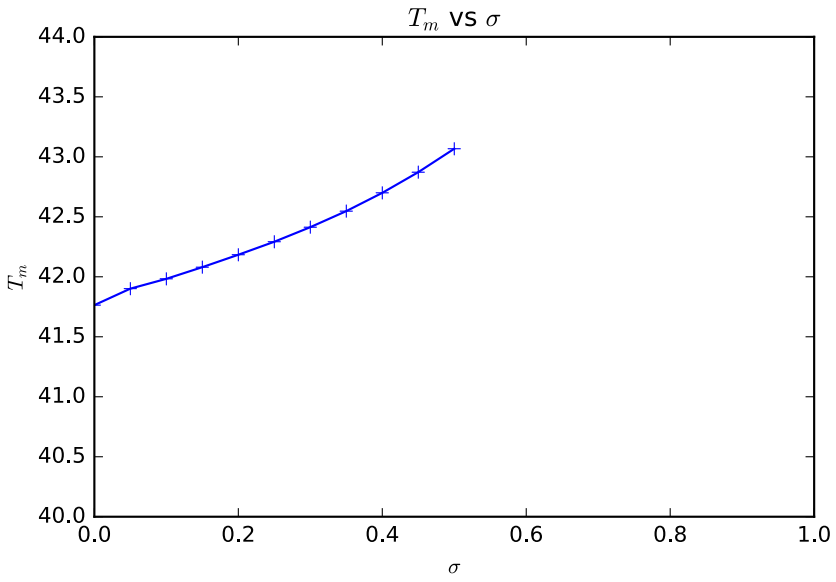

Figure S6: Variation of the apparent melting temperature (inflection point of $\Delta H(T)$)

A comparison with the usual self-consistent Ising equation $m = \tanh(\beta J_{\text{Ising}} z m)$ shows that $J = 2J_{\text{Ising}}$. One could also have deduced it from the mismatch energy associated with two antiparallel spins around a bond ($2J_{\text{Ising}}$) which equals our mismatch energy J. Eq. (S21) leads to the mean-field value $\beta J_{\text{Ising}} z = \tilde{J}/2 = 1$.

By comparison, the exact value of the critical point on a 2d hexagonal lattice Ising model is $\beta J_{\text{Ising}} = 0.2746\ldots$ (see (59), page 671). In our notations, this corresponds to $\tilde{J} = 0.5432$. Back to the original parameter J, one finds (with $z = 6$, and 1 cal=4.18 J):

- mean-field: $\mathcal{N}_A J = \frac{2}{z} RT_m = 860 \text{ J} \cdot \text{mol}^{-1} = 205 \text{ cal} \cdot \text{mol}^{-1}$,
- exact: $\mathcal{N}_A J = 2 \times 0.2746 \times RT_m = 1414 \text{ J} \cdot \text{mol}^{-1} = 338 \text{ cal} \cdot \text{mol}^{-1}$.

The mean-field approximation underestimates the magnitude of the coupling constant that is needed to correlate the spins to a given degree.

We can compare now the values used in this study to those of Jerala et al. (55). In Jerela et al., the gel-fluid mismatch penalty is noted $\omega = J$. The proposed value for fitting the DSC curve of DPPC systems is $\omega = 282$ cal, when internal degrees of freedom are associated to whole lipids. This corresponds to a ratio $J/J_c = 282/338 = 0.8343$.

Transposed to the mean-field critical value $205 \text{ cal} \cdot \text{mol}^{-1}$, this would corresponds to a $J \simeq \omega \simeq 0.8343 \times 205 = 171 \text{ cal} \cdot \text{mol}^{-1}$ (715 J ·mol^{-1}). By comparison, we use in the above approach $J = 199 \text{ cal} \cdot \text{mol}^{-1}$ (830 J·mol^{-1}) and $J' = J'' = 100 \text{ cal} \cdot \text{mol}^{-1}$ (415 J·mol^{-1}). We therefore globally operate closer to the critical point.